INFLUENCE OF THE RIGID AMORPHOUS FRACTION AND CRYSTALLINITY ON POLYLACTIDES TRANSPORT PROPERTIES

*Ainara Sangroniz[1], Ana Chaos [1], Marian Iriarte[1], Javier del Río[2], Jose-Ramon Sarasua[3], Agustin Etxeberria[1,]**

[1] POLYMAT, Department of Polymer Science and Technology, University of the Basque Country UPV/EHU, Manuel de Lardizabal, 3. 20018 Donostia (Spain).

[2] Department of Material Physics, Complutense University of Madrid, Ciudad Universitaria s/n, 28040 Madrid (Spain).

[3] POLYMAT, Department of Mining-Metallurgy Engineering and Materials Science, School of Engineering, University of the Basque Country UPV/EHU, Plaza Ingeniero Torres Quevedo 1, Bilbao, Spain.

* Correspondence to: Agustin Etxeberria (E-mail: agustin.etxeberria@ehu.es)

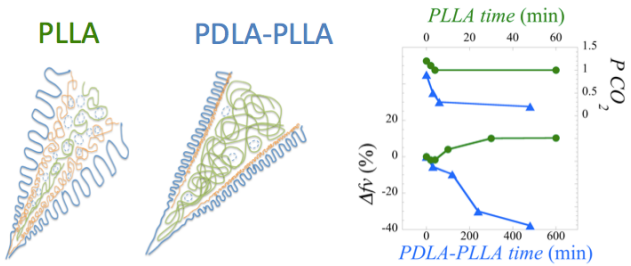

Figure for Table of Contents use only.

ABSTRACT

The effect of the crystallinity and polymorphism of PLLA and PDLA-PLLA 50:50 blends on the free volume and transport properties have been studied. In the case of PDLA-PLLA 50:50 the increase on crystallinity promotes a process of densification and a reduction in free volume fraction and rigid amorphous fraction (RAF), contrary to PLLA in which the enlargement of a rigid amorphous fraction leaded to a dedensification. This result offers a unique opportunity to analyze separately the opposite influence in the transport properties of the crystallization and free volume associated with RAF. Overall, these findings provide a better understanding on the relationship between crystallinity and transport properties and would explain also the controversial data reported in the literature.

INTRODUCTION

Crystallization and free volume are two important factors that influence the barrier properties of polymers. Crystalline regions are considered impermeable: penetrant sorption in the crystalline region could be considered negligible in comparison with the amorphous region, therefore the crystallization should reduce solubility[1,2]. Diffusivity is further affected since the crystallites create a tortuous pathway. Thus, the global process, permeability, is also reduced. Free volume plays the opposite role: as the free volume increases the permeability also rises[1,2]. Free volume is in principle reduced as crystallization grows[2].

Moreover, the segmental mobility and mechanical properties, among others, show also peculiar behavior in the crystallized samples[3]. The two-phase model cannot explain this phenomena and the coexistence of three different regions must be considered[4-7]. The non-crystalline phase must be divided in the non-crystalline

amorphous region, in other words a bulk mobile amorphous fraction (MAF), and the crystalline-amorphous interfacial regions. This amorphous region has a minor segmental mobility and is usually described as rigid amorphous fraction (RAF)[8-11]. The formation of RAF has been reported in a wide range of polymers as it has been reported in an extensive review by Wunderlich[12].

As RAF vitrifies during crystallization at superior temperatures than the glass transition temperature, an excess of free volume is also associated with the RAF region[13] leading to the so-called dedensification effect. This effect has been studied by means of positron annihilation lifetime spectroscopy (PALS) showing a larger free volume of the RAF regarding to MAF[9,14]. Also, the dedensification can explain the anomalous evolution of the gas solubility with crystallization degree[7,15,16]. For instance, annealed poly(ethylene terephthalate) and poly(ethylene naphthalate) show that the oxygen solubility is independent of crystallinity. Furthermore, an increase on the amorphous solubility as the crystallinity level rises is found, that arises from the formation of RAF[7,15,16].

In literature the relation between permeability and crystallinity for different polymers has been deeply studied in a review published by Kanehashi et al.[17]. In that work they conclude that as the crystallinity increases the diffusion, solubility and permeability decrease. However, at low crystallinity levels the diffusion and permeability can be maintained constant or even can increase for some polymers.

Regarding the transport properties of polylactide, there are many reports studying the relationship between crystallinity and permeability. Colomines et al.[18] observed that there was no relation between oxygen permeability and PLA crystallinity. Sawada et al.[19] observed that the permeability increased for crystalline polylactide respect to the amorphous one. Drieskens et al.[20] found that the increased

crystallinity reduces the permeability, but the relation is not linear. Guinault et al.[21] have studied the effect of the crystallinity level of α and α´polymorphisms on the barrier properties finding that increasing α´ fraction the permeability raises which is related to the formation of rigid amorphous phase. In another work carried out by Courgneau et al.[22] no differences were observed for the studied penetrants between α and α´polymorphisms. Sato et al.[23] have studied also the relation between the rigid amorphous fraction and permeability concluding that as the rigid amorphous fraction increases the diffusivity and permeability decrease. Recently Fernandes et al.[24] have studied the effect of the crystalline structure and rigid and mobile amorphous fractions on oxygen permeability. They have concluded that the rigid amorphous fraction is the factor that plays the major role on the oxygen diffusion coefficient while the solubility is more affected by the crystallinity level. They propose that an excess free volume is created near the crystals, thus, as the rigid amorphous fraction increases more free volume is generated, which is in agreement with our previous work[25]. Regarding crystalline structure Bai et al.[26] obtained PLA with shish-kebab-like crystals and they achieved a great reduction on oxygen permeability.

The rigid amorphous fraction of poly(L-Lactide) (PLLA) crystallized in the α polymorph was reported using differential scanning calorimetry, among others[5,27-30]. Later, a complete characterization of the free volume was carried out on basis of PALS[25]. The main features for this work were the reduction of the free volume hole but the increase of the hole number leading to an increased free volume fraction as the rigid amorphous fraction (RAF) rose up with crystallization degree. In the case of polylactide, the equimolecular mixture of PDLA and PLLA stereoisomers allows to obtain the crystallization in the so-called stereocomplex polymorph. More compact side-by-side crystallization between the two enantiomeric polymers results in a much

higher melting temperature being approximately 50 ºC superior to the corresponding homocrystal α polymorph[29,31]. A stereocomplex racemic crystallite having 3/1 helical structure is different of the homopolymer crystallite with 10/3 helical structure found in individual PLLA[32].

When the amorphous phase of PDLA-PLLA 50:50 mixture was studied, as we will show later in this paper, we realized that RAF was not observed in the stereocomplex, unlike what happens with PLLA homocrystals. This result offers a unique opportunity to compare the opposite influence of the crystallization and excess free volume associated to RAF in the transport properties.

EXPERIMENTAL PART

Sample preparation and thermal treatments

PLLA was supplied by Biomer® (Germany) and has an average number molecular weight (Mn) of 153000 g/mol and a polydispersity index (Mw/Mn) of 1.38, as determined by GPC. It contains 2 % D-lactyl moieties and 0.2 % residual monomer, according to the supplier. PDLA was purchased from Purac Biochem and has an average weight molecular weight of 349000 g/mol and the polydispersity index is of 1.92. According to the supplier it contains 2 % L-lactyl moieties and 0.2 % residual monomer. Their properties are shown in the Table 1.

Table 1. Properties of PLLA and PDLA polymers.

Polymer	Mn (g/mol)	Polydispersity index	L-LA (%)	D-LA (%)	Residual monomer (%)
PLLA	153000	1.38	98	2	0.2
PDLA	349000	1.92	2	98	0.2

PLLA pellets were dried overnight in a vacuum oven at 30 ºC prior to processing and afterwards conformed in sheets of 100 mm x 100 mm x 1 mm by hot-pressing at 180 ºC under a pressure of 4 bar for the first minute and 240 bar for additional 4 min. Solidification was carried by moving away the sheet from the mold and sinking it in a water bath (water-quenching, WQ). The compression-molded sheets were cut in smaller sheets of 10 mm x 10 mm x 1 mm, and were annealed in an oven. Thermal treatments were carried out at 100 ºC during 2, 4, 10, 15, 30 and 60 minutes in order to obtain samples containing different crystalline and rigid amorphous fractions.

In the case of PDLA-PLLA 50:50 samples, the blend was prepared by casting in chloroform from 2 wt % solutions. After the evaporation of the solvent the films were treated in a press at 230 °C. The solidification was performed as in the previous case employing a water bath. Finally, the thermal treatment was carried out at 190 ºC during 15, 30, 60, 120, 240, 480 and 720 minutes in order to obtain samples with different crystallinities. As in the previous case the sheets have a thickness of 1 mm, which have been used for DSC and PALS measurements.

Membranes of 20-60 μm thickness of PLLA and PDLA-PLLA 50:50 blends were prepared following the above-mentioned procedures in order to carry out both the permeability and sorption measurements.

Positron lifetime measurements

Positron annihilation measurements were performed employing a ^{22}Na positron source deposited onto a thin Kapton© foil. This positron source was placed between two identical PLLA samples of 1 mm in thickness. The positron lifetime spectra were recorded at room temperature by using a conventional fast-fast nuclear spectrometer with a time resolution (FWHM) of 230 ps. For each measurement the average of three

spectra with 2×10^6 total counts were registered and analyzed by using the standard program PATFIT-88. More details about the procedure were described elsewhere[25,33]. Positron lifetime spectra have been fitted by using three exponential decays and the longest time component has been associated to ortopositronium (o-Ps) lifetime formed into free volume holes of sample. The positron annihilation in the free-volume holes makes it possible to correlate the hole dimension with their measured lifetime. According to the model proposed by Eldrup[34], the o-Ps lifetime is related to the free volume hole radius, R, by:

$$\tau_{O-Ps} = 0.5\left(1 - \frac{R}{R_0} + \frac{\sin\left(2\pi\frac{R}{R_0}\right)}{2\pi}\right)^{-1} \quad (1)$$

where $\tau_{o\text{-}Ps}$ is given in nanoseconds and $R_0 = R + \Delta R$. The radius ΔR is an empirical parameter and the best value obtained by fitting all known data is 1.656 Å[35]. The mean free volume hole size, V_H, assuming a spherical form for the holes, may be estimated by using a simple equation:

$$V_H = \left(4\pi \cdot R^3\right)/3 \quad (2)$$

The relative intensity corresponding to the longest component present in the spectra and associated to the o-Ps annihilation in the free volume holes, $I_{o\text{-}Ps}$, is related to the number of the free volume holes. Furthermore, combining the number ($I_{o\text{-}Ps}$) and size of free volume holes (V_H), the fractional free volume (f_v) could be extracted by[36]:

$$f_v = cV_H I_{O-Ps} \quad (3)$$

where c is a characteristic constant of each material, but it is difficult to know the value of c for many polymers. Moreover, there are other factors, besides the number of the free volume holes that influence in $I_{o\text{-}Ps}$[37].

As in the previous paper[25], in order to obviate c and taking into account that we are more interested in the evolution of f_v with annealing than in its absolute value, in this work we have used the free volume fraction increment defined as:

$$\Delta f_v = \left(f_v^t - f_v^Q \right) \Big/ f_v^Q \tag{4}$$

where f_v^t is the free volume fraction after an annealing time of t minutes and f_v^Q is the free volume fraction in the as-quenched state.

Differential Scanning Calorimetry

Differential scanning calorimetry (DSC) was conducted on a DSC 2920 thermal analyzer from TA Instruments. Samples of approximately 5 mg were encapsulated in aluminum pans. The scans were performed from 0 °C to 250 °C at 10 °C/min heating rate.

The fractions of crystalline phase (X_c), stereocomplex (X_S), mobile amorphous fraction (X_{MA}, MAF) and rigid amorphous (X_{RA}, RAF) fraction in PLLA were determined according to a procedure described in a previous work employing Equations 5-11,

$$X_c(\%) = \frac{\Delta H_{m,H} + \Delta H_{m,S} - \Delta H_{c,H}}{\Delta H^0_{m(blend)}} \times 100 \tag{5}$$

$$\Delta H^0_{m,blend} = w_H \Delta H^0_{m,H} + w_S \Delta H^0_{m,S} \tag{6}$$

where w_H and w_S are defined as follow,

$$w_H = \frac{\dfrac{\Delta H_{m,H} - \Delta H^0_{c,H}}{\Delta H^0_{m,H}}}{\dfrac{\Delta H_{m,H} - \Delta H_{c,H}}{\Delta H^0_{m,H}} + \dfrac{\Delta H_{m,S}}{\Delta H^0_{m,S}}} \tag{7}$$

$$w_S = \frac{\dfrac{\Delta H_{m,S}}{\Delta H^0_{m,S}}}{\dfrac{\Delta H_{m,H} - \Delta H_{c,H}}{\Delta H^0_{m,H}} + \dfrac{\Delta H_{m,S}}{\Delta H^0_{m,S}}} \tag{8}$$

$$X_S = \frac{\Delta H_{m,S}}{\Delta H^0_{m,S}} \times X_c \quad (9)$$

$$X_{MA} = \frac{\Delta c_p}{\Delta c^0_p} \quad (10)$$

$$X_{RA} = 1 - X_c - X_{MA} \quad (11)$$

where $\Delta H_{m,H}$, $\Delta H_{m,S}$ and $\Delta H_{c,H}$ are the experimental values of melting enthalpy of α form crystals and stereocomplex crystals, cold crystallization and crystallization just before the melting of PLA crystals; $\Delta H^0_{m,H}$ and $\Delta H^0_{m,S}$ are the theoretical values of the melting enthalpy of 100 % homocrystalline PLLA, 106 J/g[28], and the 100 % stereocomplex, 142 J/g[28], and (Δc_p) and (Δc^0_p) are the experimental specific heat changes at T_g of PLLA and PDLLA respectively, the later giving account for the specific heat change at T_g of the non-confined mobile fully amorphous phase, Δc^0_p = 0.639 J/(g K)[38].

Density measurements

The density of the samples were measured using a gradient density column. The measurements were performed using NaBr aqueous solution at 23 °C. Three samples were characterized for each material.

Transport measurements devices

Carbon dioxide sorption kinetics were measured employing a Hiden IGA-2 electrobalance. The measurements were performed at 1, 5, 10, 15 and 20 atm and 30 °C. After the appropriate data treatment of the sorption kinetic, both solubility and diffusion coefficients (*S* and *D*, respectively) can be determined. The absorbed gas concentration (*C*) was calculated from the equilibrium weight gain (M_∞) of the membrane by means of the following equation:

$$C\left[\frac{\text{cm}^3\ \text{STP}}{\text{cm}^3}\right]=\frac{22414\cdot M_\infty}{44\cdot V_{plm}} \tag{12}$$

where V_{plm} is the volume occupied by the sample, in cm^3; M_∞, the total absorbed mass at equilibrium in g; and 44 g/mol, the molecular weight of CO_2. Then, the solubility coefficient S is given by this simple equation:

$$S=\frac{C}{p} \tag{13}$$

being p the pressure. In order to obtain the diffusion coefficient, Fick's second law must be solved, which depends on the geometry and concentration conditions. For a thin film geometry in which the diffusion from the edge of the film is considered negligible and assuming that the pressure of the penetrant and the diffusion coefficient are constant, the mass uptake of the penetrant can be described by [39]:

$$\frac{M_t}{M_\infty}=1-\frac{8}{\pi}\sum_{n=0}^{\infty}\frac{1}{\left(2n+1\right)^2}\exp\left(-\frac{D\left(2n+1\right)^2\pi^2 t}{l^2}\right) \tag{14}$$

where M_t is the absorbed gas at t time; l, the film thickness; and D, the diffusion coefficient (in cm^2/s). This equation can be simplified leading to the so-called short time (up to 50% of M_∞) and long time approximation (50-90 % of M_∞).

The oxygen permeability coefficient was measured employing a Mocon OX-TRAN 2/21 MH model equipment at 1 atm, 30 °C and 0 % relative humidity. Its software gives directly the oxygen transmission rate (*OTR*), which can be easily transformed to the permeability coefficient, in Barrer, by:

$$OTR\left(\frac{cm^3}{m^2.day}\right)\cdot l\cdot\frac{0.29398}{p\left(mmHg\right)}=P(Barrer) \tag{15}$$

Water vapor transmission rate measurements were carried out using a permeation gravimetric cell. The cell, made in polytetrafluoroethylene, is basically a small container partially filled with the corresponding penetrant, water in our case, sealed by a polymer membrane. This cell is placed on a Sartorius balance with a 10^{-5} g readability. Weight loss is monitored and recorded on a computer for further data treatment[40]. The results shown are the average of at least three measurements. The measurements were carried out at 30 °C. In this case, water vapor transmission rate, *WVTR* (g mm/m^2 day), can be written as:

$$WVTR = \frac{Q}{s}\frac{l}{\left(1 - a_{out}\right)} \tag{16}$$

where Q is the slope of the permeated mass *versus* time plot, s is the exposed area of the film (2.54 cm^2 in this case) and a_{out} can be calculated from relative humidity of the surrounding ambient, measured using a Delta OHM thermohygrometer.

More details about the precedent techniques and operation procedures appear in previous works[41-43].

RESULTS AND DISCUSSION

Thermal properties

Taking into account the effect of the annealing treatment in the crystallinity and rigid amorphous fraction of PLLA it is interesting to analyze the effect of the annealing on the stereocomplex. Figure 1 shows the DSC heating thermograms of PDLA-PLLA 50:50 samples. As it can be seen PDLA-PLLA sample obtained by water quenching shows the glass transition temperature at 60 °C, cold crystallization at 118 °C and two melting peaks: one located at 180 °C, corresponding to the melting of the optically pure polymer, and another one at 219 °C, corresponding to the melting of the stereocomplex. The glass transition temperature has been determined

from the midpoint of the heat capacity change and the cold crystallization and melting temperature from the minimum and maximum of the peak, respectively. For the blends crystallized at 190 °C for different times it can be observed that increasing the annealing time the cold crystallization enthalpy decreases, the melting enthalpy of the optically pure homopolymer decreases and the melting enthalpy of the stereocomplex increases. The glass transition temperature varies slightly with the annealing time until 240 min when it starts to decrease due to the reduction of RAF, see Figure S1 in Supporting Information. For the samples annealed for 240 and 480 min the heat capacity change decreases considerably due to the higher crystallinity.

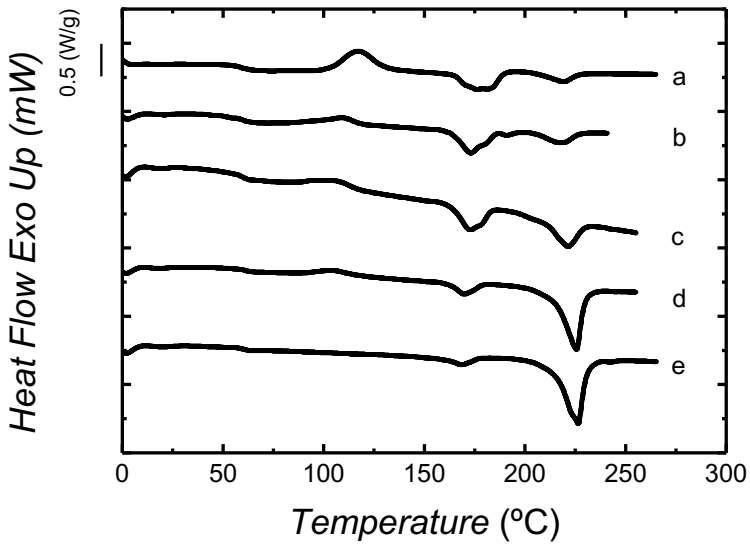

Figure 1. DSC heating thermograms of PDLA-PLLA 50:50 samples obtained by a) water quenching b) crystallized at 190 °C 30 min c) 1 h d) 4 h e) 8 h and f) 12 h.

In Figure 2 a) and b) the crystallinity fraction, RAF and MAF are shown for PDLA-PLLA 50:50 and PLLA samples, respectively, annealed for different times. As can be seen, for PDLA-PLLA 50:50 the crystallinity raises with the annealing time until 180 minutes, after that it is maintained constant. The stereocomplex fraction also follows a similar trend increasing with the annealing time until 180 min achieving 90

% of the global crystalline fraction. The rigid amorphous fraction suffers small variations and after 240 min it decreases considerably. The mobile amorphous fraction is reduced as the crystallinity increases and after 240 min small changes occur. Since the crystallinity is maintained constant, these changes are counterbalanced by the rigid amorphous fraction.

Regarding PLLA we summarize the previously reported data of thermal characterization[25]. Water quenched PLLA is practically amorphous and with annealing treatment the crystallinity raises considerably. The rigid amorphous fraction increases with crystallinity and the mobile amorphous fraction is decreased, see the Figure 2 below. The glass transition temperature increases considerably with the increased crystallinity, see Figure S1 in supporting information, that is attributed to the coupling between the crystals and amorphous phase inside the crystals[24,44-46]. As it can be observed in the glass transition temperature vs annealing time figures the T_g increases for PLLA whereas in the case of PDLA:PLLA by the end a reduction is observed. These results have to be analyzed carefully since the glass transition temperature varies slightly from one measurement to another, but it seems clear that the decrease of the T_g is related to the reduction of RAF. The Δc_p step is associated to the mobile amorphous fraction. The step decreases, when increasing annealing time, that can be due to the increase of the crystallinity as well as to the generation of the rigid amorphous phase.

Therefore, a great difference is observed between PLLA and PDLA-PLLA 50:50: although the crystallinity rises in both cases the rigid amorphous fraction increases for PLLA whereas for PLLA-PDLA is decreased. The result is surprising and it could be due to the fact that two polymer chains, PDLA and PLLA, are involved in the stereocomplex formation. We will discuss this point later.

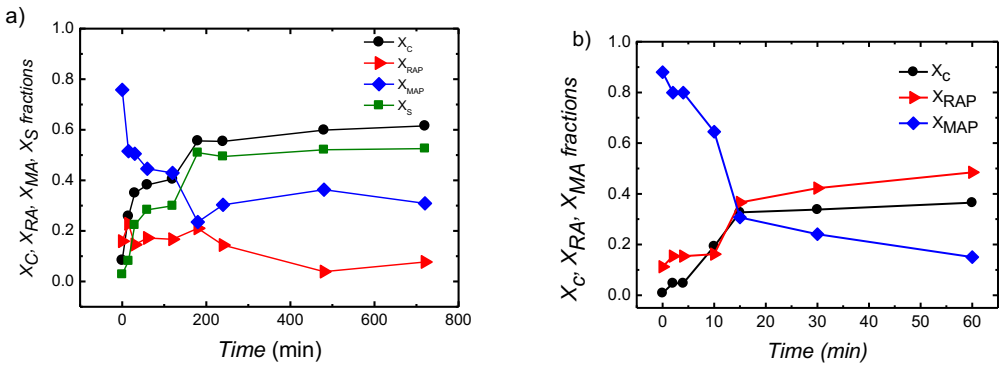

Figure 2. Global crystallinity, X_c, stereocomplex crystallinity, X_S, rigid amorphous fraction, X_{RAF}, and mobile amorphous fraction, X_{MAF}, for a) PDLA-PLLA 50:50 and b) PLLA samples.

Free volume characterization

Regarding free volume, PDLA-PLLA 50:50 sample shows that both, $\tau_{o\text{-}Ps}$ and $I_{o\text{-}Ps}$, decrease with annealing time, see Figure 3 a). The overall free volume fraction, see Figure 4, decreases which is in accordance with the data obtained from the DSC, where the rigid amorphous fraction is small. Similar findings were obtained for melt-crystallized PET[14]. It is worth to note that the behavior observed for PDLA-PLLA 50:50 is the opposite to that observed for PLLA.

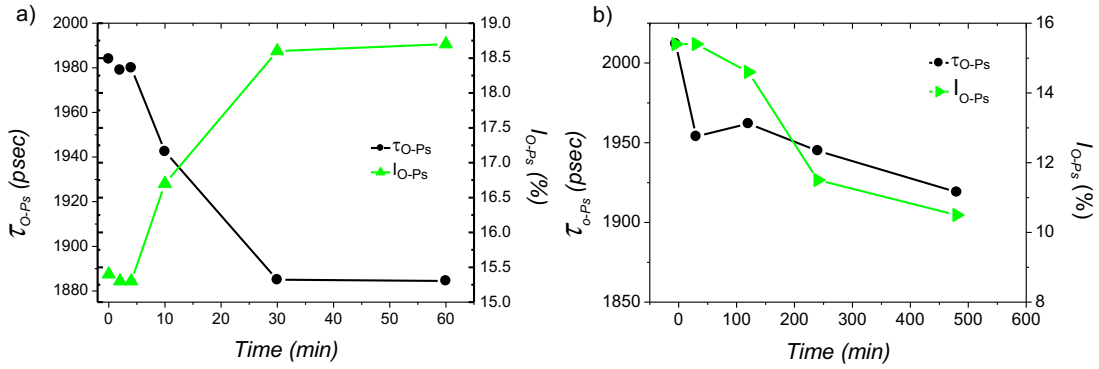

Figure 3. o-Ps annihilation lifetime, $\tau_{o\text{-}Ps}$, and o-Ps annihilation intensity, $I_{o\text{-}Ps}$, of a) PLLA and b) PDLA-PLLA 50:50 blends.

In the case of PLLA o-Ps annihilation lifetime decreases with the annealing time while the o-Ps annihilation intensity increases, see Figure 3 b). This indicates

that the increase of the rigid amorphous fraction leads to a decreased free volume hole size and an increased number of holes. The free volume fraction that encompasses both factors increases with the annealing time which is in good agreement with the data reported for other semicrystalline polymers. Therefore, it was concluded in our previous work that in the rigid amorphous phase the chains adopted a more rigid and extended conformation than in the mobile amorphous phase leading to a higher free volume[25].

The differences observed for PLLA and PDLA-PLLA 50:50 may arise from different factors: for PDLA-PLLA 50:50 a) the crystalline structure is more compact since it contains two polylactide chains b) the density of the tie chains is higher[47] c) the crystallization process is conducted for a longer time therefore the chains have time to reorganize reducing the excess free volume d) in our opinion, the lack of RAF formation in the stereocomplex could derive from the fact that the two chains which leave the crystalline region would create an amorphous domain with enough size to assure the mobility of the segment located in this amorphous region avoiding the generation of the RAF.

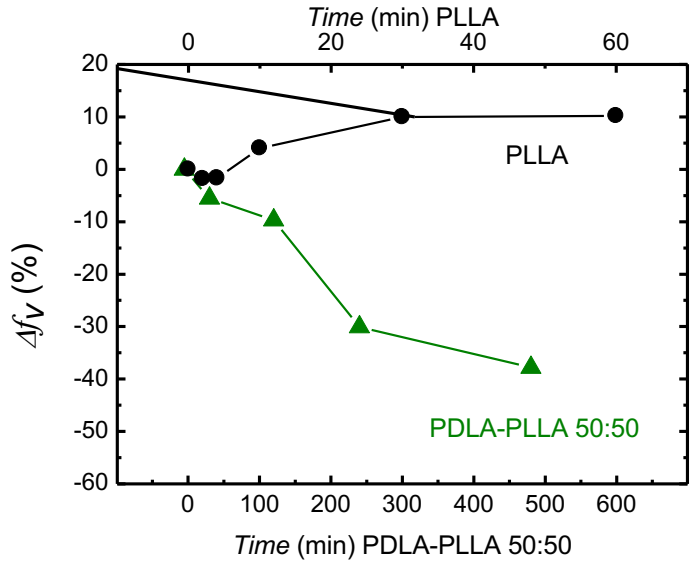

Figure 4. Free volume fraction of PLLA and PLLA-PDLA 50:50 blend.

Density measurements

Taking into account that RAF and crystallinity have opposite effect in the density, density measurements would clarify what factor is playing the major role on both PLLA and PDLA-PLLA 50:50 samples. Table 2 shows the density values for PLLA and PDLA-PLLA 50:50 at different annealing times.

According to density measurements a dedensification occurs for PLLA with the increasing of the rigid amorphous fraction. This is due to the confinement of the amorphous chains that are anchored to crystallites leading to a lower density of the interlamellar amorphous region[7,15]. This effect overcomes the densification associated to a major crystalline fraction. On the contrary, PDLA-PLLA 50:50 shows a densification process as the annealing time increases. The obtained results are in good agreement with the data obtained for the free volume fraction.

Table 2. Density values for PLLA and PDLA-PLLA 50:50 samples at different annealing times.

Sample	Annealing time (min)	ρ (g/cm^3)	Sample	Annealing time (min)	ρ (g/cm^3)
PLLA	0	1.2468	PDLA-PLLA 50:50	0	1.2567
PLLA	2	1.2554	PDLA-PLLA 50:50	30	1.2588
PLLA	4	1.2432	PDLA-PLLA 50:50	60	1.2643
PLLA	60	1.2411	PDLA-PLLA 50:50	480	1.2704

In the previous sections it has been observed that the annealing treatment provokes changes in the crystallinity, rigid amorphous fraction and free volume. Density measurements also show that the excess free volume associated with rigid amorphous fraction could balance out, even overcome, the reduction of the free volume fraction associated to the increase of the crystallization. It is expected that these changes would affect transport properties, therefore in the following section sorption of carbon dioxide and the permeability to different gases and vapors are analyzed.

Transport properties

Sorption measurements

Carbon dioxide sorption isotherms for PLLA and PDLA-PLLA 50:50 samples with different thermal treatments are shown in Figure 5 a) and b), respectively, the data is reported in Table S1 and S2 in supporting information. As can be seen, PLLA without treatment and PLLA annealed for 2 min present a CO_2 concentration that is proportional to the pressure at low pressures, that is, follows Henry´s law. However, as the pressure increases the isotherm shows a curvature and it is well fitted to the dual model which is a combination of Henry and Langmuir type isotherm. This behavior is usual in polymers that have a glass transition temperature above measurement temperature. Moreover, no differences have been observed between PLLA without treatment and PLLA annealed for 2 min.

For PLLA annealed for 60 min, at low pressures the concentration of carbon dioxide is slightly lower than for the other two samples due to the higher crystallinity level of PLLA 60 min, since sorption does not occur in the crystals. However, for pressures higher than 15 bar the isotherm turns up. This behavior could arise from two facts. For this sample the rigid amorphous fraction is higher than in the other samples

but the associated excess free volume could be trapped between the crystals. Therefore, it could be concluded that this excess free volume is not easily available and only at very high pressures the carbon dioxide could access to this free volume. Due to the large excess free volume a sharp increase in the carbon dioxide concentration is obtained. The second fact is the well known plasticization effect of carbon dioxide[48]. This effect could also be enhanced due to the large excess free volume.

PDLA-PLLA 50:50 sample without treatment shows a dual mode sorption and the data obtained is very similar to PLLA. However, the sample annealed for 30 min shows a very different behavior: a Henry type sorption is obtained. For this sample, as it has been pointed out above, large quantity of stereocomplex is formed being its apparent free volume fraction low. Thus, it would deduce that the excess free volume decrease could lead to diminish the Langmuir type sorption sites, thus the isotherm obtained follows apparently Henry´s law.

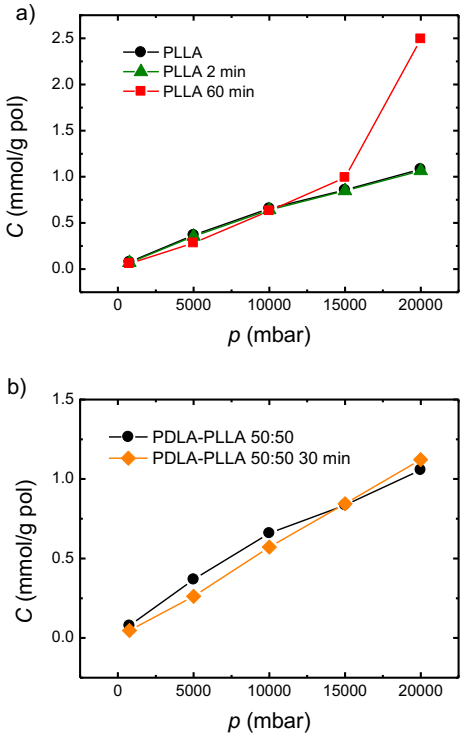

Figure 5. Carbon dioxide sorption isotherms for a) PLLA and b) PDLA-PLLA 50:50 samples with different thermal treatments.

In order to analyze the effect of the crystallinity and rigid amorphous fraction on the solubility, *S*, the solubility referred to the amorphous part, S_{am}, and the diffusion coefficient, *D*, for PLLA and PDLA-PLLA 50:50 are shown in Figure 6.

PLLA shows that the diffusion coefficient is maintained constant over the different crystallinities. *A priori* the diffusion coefficient has to decrease with the increased crystallinity since the crystals form a tortuous pathway. Although in this case the crystallinity goes from 4 % of PLLA 2 min to 36.5 % for PLLA 60 min the diffusion coefficient is maintained constant. However, the free volume increases which would lead to a higher diffusion coefficient. Therefore, the behavior of the diffusion coefficient could be attributed to the counterbalance of the two effects.

The solubility, *S*, is decreased with the increase of the crystallinity since the penetrants cannot be solubilized on the crystals. However, the amorphous solubility, S_{am}, increases which is not the expected behavior since it would be maintained constant. This result could be related to the excess free volume generated in the rigid amorphous phase.

On the other hand, PDLA-PLLA 50:50 shows a completely different behavior: the diffusion coefficient is decreased due to the increment of the crystallites since the excess free volume associated to RAF cannot balance as occurs in the PLLA case. The overall solubility, *S*, is also decreased due to the presence of the crystals whereas S_{am} is maintained constant. This is the expected behavior with the crystallinity in a two-phase model of crystallization, i.e. in absence of RAF. The obtained results for solubility and diffusion coefficient are in good agreement with the data obtained by Fernandes et al.[24] for PLA in which permeability, solubility and diffusion coefficients

to oxygen decreased with crystallinity until a certain limit. They found that after this limit it increases due to the increase in the RAF.

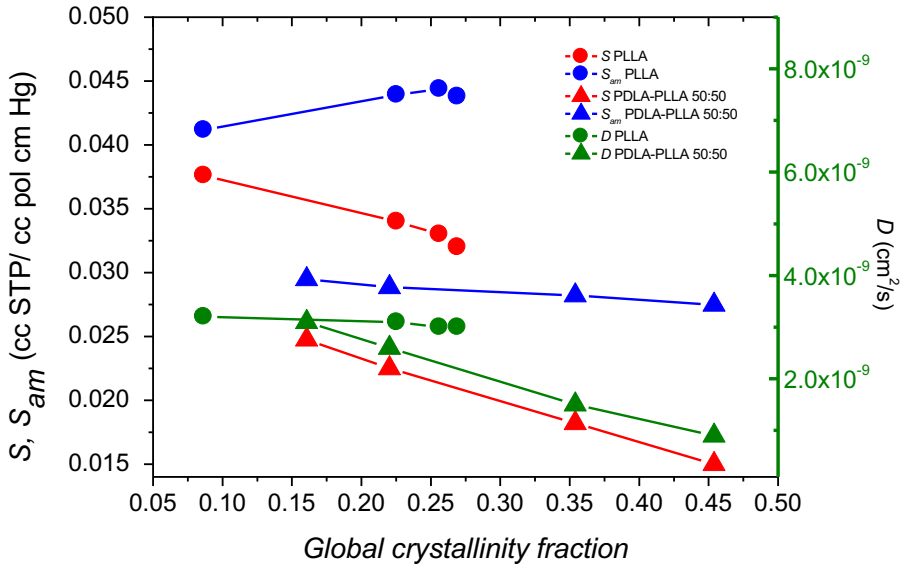

Figure 6. Carbon dioxide solubility, *S*, amorphous solubility, S_{am}, and diffusion coefficient, *D*, for PLLA and PDLA-PLLA 50:50 samples.

Permeability

In Figure 7 a) the permeability to oxygen, b) carbon dioxide and c) the water vapor transmission rate for PLLA and PDLA-PLLA 50:50 samples that have been annealed for different times are shown, the permeability coefficients values are reported in Table S3 and S4.

Regarding PLLA, the permeability of oxygen is reduced as the annealing time increases due to the increase of the crystallinity and the decrease of the mobile amorphous fraction. The sample obtained by water quenching and the sample annealed for 2 min show similar permeability values. It can be suggested that this arises from the counterbalance effect of crystallinity and excess free volume. Despite the increase of the free volume, the permeability is curiously reduced for the sample annealed for 60 min. The size of the free volume holes is reduced whereas the number

of holes increases, and the results indicate that the reduction of the free volume hole size would be playing a major role on the permeability as well as the possible inaccessibility of the created free volume in the rigid amorphous fraction, as mentioned above.

Carbon dioxide permeability values have been calculated by the following equation: $P = D \cdot S$ where diffusion and solubility are obtained by sorption experiments. In this case the reduction of the permeability is smaller than that observed for O_2. Carbon dioxide has a higher critical volume than oxygen and taking into account the reduction of the size of the free volume holes this is not the expected behaviour. Probably the more interacting character of carbon dioxide, as well as, the presence of a large number of holes can promote a quicker diffusion process. Moreover, as mentioned above, carbon dioxide could act as a plasticizer, even though this phenomenon is observed at higher pressure, the presence of a large number of holes could facilitate the plasticization process. Both events would lead to a greater permeability than expected, overcoming the effect of the reduction in the size of the free volume holes.

The water vapor transmission rate shows that the permeability is decreased as the crystallinity increases. However, for the sample annealed for 60 min a higher value than expected one is obtained, the increase of the free volume counter balance the effect of the crystallinity. Water molecules can also provoke the plasticization of the polymer leading to a higher permeability values. The differences between the studied three penetrants arise from the more interacting character of water that can form hydrogen bonds and dipole-dipole interactions whereas oxygen and carbon dioxide form only weak van der Waals interactions.

Overall, the reduction found in the permeability for the different penetrants arises from two factors: the crystallinity and free volume. In PLLA the crystallinity and rigid amorphous fraction increased whereas the mobile amorphous fraction decreased with the thermal treatment. The crystals are impermeable, therefore they increase the tortuosity decreasing the diffusion coefficient. The solubility is also decreased since it is considered that penetrants can not be solubilized in the crystals. The other effect that has to be considered is the free volume that increases with the annealing time, but part of the free volume could be inaccessible for penetrants at low pressures. Furthermore, the formation of RAF increases the free volume since the polymer chains are more extended and have a more rigid conformation than in MAF[25]. Taking into account that the permeability is reduced it can be concluded that the crystallinity plays a major role even though free volume influence can be also observed.

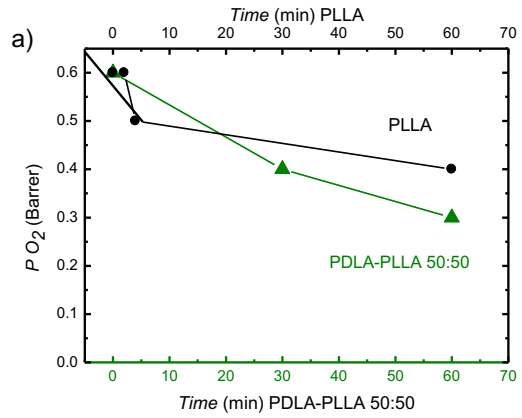

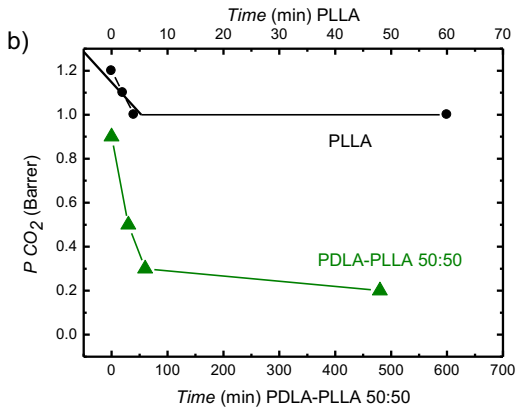

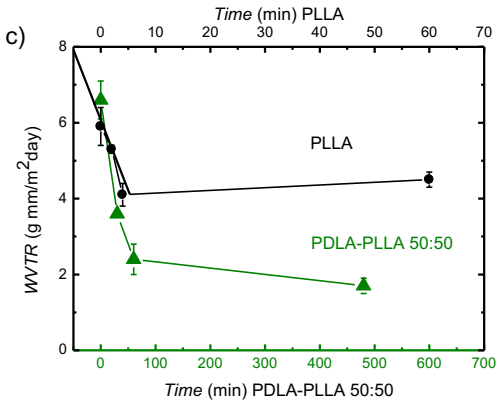

Figure 7. a) Oxygen permeability, b) carbon dioxide permeability and c) water vapour transmission rate for PLLA and PDLA-PLLA 50:50 samples with different annealing times.

Regarding PDLA-PLLA 50:50 samples, the permeability to oxygen is decreased considerably with the annealing time since the crystallinity and the stereocomplex formation increases. The reduction of the rigid amorphous fraction, which has a higher free volume, also has a positive effect on the barrier properties. The results are in accordance with free volume measurements where a reduction is found with the annealing time. In the case of carbon dioxide and water vapor the reduction is similar for both penetrants and higher than for oxygen.

For PDLA-PLLA 50:50 the permeability reduction is directly related to the formation of the stereocomplex and the reduction of the rigid amorphous fraction (RAF). Both, the increase of the crystallinity and reduction of RAF contribute to the reduced permeability, as explained before. The obtained results are in good agreement with the hypothesis proposed by del Rio et al.[25] and the data obtained by Fernandes et al.[24] for the oxygen permeability of PLA.

Comparing the two systems the permeability reduction is higher for PDLA-PLLA 50:50 than for PLLA, which arises from the increase of crystallinity and the no

formation of RAF. The improvement obtained with the stereocomplex is not comparable to that reported by Bai et al.[26] who obtained an outstanding improvement on the barrier properties of PLA with shish-kebab crystallization. In any case the stereocomplex presents a lower permeability than PLLA. Furthermore, for PLA Fernandes Nassar et al.[24] obtained a greater improvement than that obtained for PLLA in this work. In any case, PDLA-PLLA 50:50 blends show a higher decrease on permeability than PLLA therefore, it could be suggested that employing different thermal treatments a higher improvement could be obtained. Overall, it can be concluded that the generation of RAF balances out the influence of the crystallinity in many properties of semicrystalline materials such as free volume fraction, density as well as transport properties.

CONCLUSIONS

In this work the effect of the crystallinity and rigid amorphous fraction on polylactide and its barrier properties have been studied. It has been observed that for PLLA as the annealing time increases the crystallinity fraction and RAF rises. Also, the samples are dedensified and the free volume fraction increases due to the presence of RAF. The permeability to water vapor, oxygen and carbon dioxide decreased slightly. The sorption measurements show that diffusion is maintained constant and the amorphous solubility rises with the increased crystallinity level due to the presence of RAF.

In the case of PDLA-PLLA 50:50 the rigid amorphous fraction is very small and it decreases with the annealing time. The density of the samples increases and the free volume fraction decreases with the crystallinity level. Regarding transport properties the permeability to the studied three penetrants is decreased considerably with the crystallinity. Finally, sorption measurements show that diffusion is decreased

proportionally to crystallinity level and amorphous solubility is maintained constant with crystallinity, which is the expected behavior for crystallized samples in two-phase model.

Overall, the comparison of the results obtained for PLLA and PDLA-PLLA 50:50 clarify the counteracted effect of the crystallinity and RAF on transport properties. This fact would explain controversial data reported in the literature. These findings allow a better understanding not only of the transport properties, but also of other properties where crystallinity and free volume play an important role such as mechanical properties, among others.

Acknowledgements

Financial support from the Basque Country Government (IT-618-13) and the Spanish Ministry of Innovation and Competitiveness MINECO (MAT-2016-78527-P) is greatly acknowledged. A.S. thanks the Basque Government for the PhD thesis grant.

Supporting information

Figure S1 and Tables S1-S4: Glass transition temperature for PLLA and PDLA-PLLA for different annealing times, carbon dioxide sorption concentration for PLLA and PDLA-PLLA 50:50, permeability coefficients of water vapor, oxygen and carbon dioxide for PLLA and PDLA-PLLA 50:50.

Author information

Corresponding author: E-mail: agustin.etxeberria@ehu.es. ORCID: Agustin Etxeberria: 0000-0001-6836-4685.

References

[1] Michaels, A. S.; Parker, R. B.; Sorption and Flow of Gases in Polyethylene. J. Polym. Sci. 1959, 41, 53-71.

[2] Klopffer, M.H.; Flaconnèche, B.; Transport Properties of Gases in Polymers: Bibliographic Review. Oil Gas Sci. Technol. 2001, 56, 223–244.

[3] Magoń, A.; Pyda, M.; Study of Crystalline and Amorphous Phases of Biodegradable Poly(lactic acid) by Advanced Thermal Analysis. Polymer 2009, 50, 3967-3973.

[4] Menczel, J.; Wunderlich, B.; Heat capacity hysteresis of semicrystalline macromolecular glasses. J. Polym. Sci.: Polym. Phys. Ed. 1981, 19, 261-264.

[5] Iannace, S.; Nicolais, L.; Isothermal Crystallization and Chain Mobility of Poly (L -lactide), J. Appl. Polym. Sci. 1997, 64, 911–919.

[6] Chen, H.; Cebe, P. Vitrification and Devitrification of Rigid Amorphous Fraction of PET During Quasi-isothermal Cooling and Heating. Macromolecules 2009, 42, 288-292.

[7] Hu, Y. S.; Liu, R. Y. F.; Zhang, L. Q.; Rogunova, M.; Schiraldi, D. A.; Nazarenko, S.; Hiltner, A.; Baer, E.; Oxygen Transport and Free Volume in Cold-Crystallized and Melt-Crystallized Poly(ethylene naphthalate). Macromolecules 2005, 35, 7326-7337.

[8] Suzuki, H.; Grebowicz, J.; Wunderlich, B.; Glass Transition of Poly(oxymethylene). Polym. Int. 1985, 17, 1-3.

[9] Dlubek, G.; Sen Gupta, A.; Pionteck, J.; Häßler, R.; Krause-Rehberg, R.; Kaspar, H.; Lochhaas, K. H.; Glass Transition and Free Volume in the Mobile (MAF) and Rigid (RAF) Amorphous Fractions of Semicrystalline PTFE: a Positron Lifetime and PVT Study. Polymer 2005, 46, 6075-6089.

[10] Androsch, R.; Wunderlich, B.; The Link Between Rigid Amorphous Fraction and Crystal Perfection in Cold-crystallized Poly(ethylene terephthalate). Polymer 2005, 46, 12556.

[11] Ma, Q.; Georgiev, G.; Cebe, P.; Constraints in Semicrystalline Polymers: Using Quasiisothermal Analysis to Investigate the Mechanisms of Formation and Loss of the rigid Amorphous Fraction. Polymer 2011, 52, 4562-4570.

[12] Wunderlich, B.; Reversible Crystallization and the Rigid-amorphous Phase in Semicrystalline Macromolecules. Prog. Polym. Sci. 2003, 28, 383-450.

[13] Schick, C.; Dobbertin, J.; Pötter, M.; Dehne, H.; Hensel, A.; Wurm, A.; Ghoneim, A. M.; Weyer, S.; Separation of Components of Different Molecular Mobility by Calorimetry, Dynamic Mechanical and Dielectric Spectroscopy. J. Thermal Anal. 1997, 49, 499-511.

[14] Olson, B. G.; Lin, J.; Nazarenko, S.; Jamieson, A. M.; Positron Annihilation Lifetime Spectroscopy of Poly(ethylene terephthalate): Contributions from Rigid and Mobile Amorphous Fractions. Macromolecules 2003, 36, 7618-7623.

[15] Lin, J.; Shenogin, S.; Nazarenko, S.; Oxygen Solubility and Specific Volume of Rigid Amorphous Fraction in Semicrystalline Poly(ethylene terephthalate). Polymer 2002, 43, 4733-4743.

[16] Hu, Y.S.; Hiltner, A.; Baer, E.; Improving Oxygen Barrier Properties of Poly(ethylene terephthalate) by Incorporating Isophthalate. II. Effect of Crystallization. J. Appl. Polym. Sci. 2005, 98, 1629-1642.

[17] Kanehashi, S.; Kusakabe, A.; Sato, S.; Nagai, K.; Analysis of Permeability; Solubility and Diffusivity of Carbon Dioxide; Oxygen; and Nitrogen in Crystalline and Liquid Crystalline Polymers. J. Membr. Sci. 2010, 365, 40-51.

[18] Colomines, G.; Ducruet, V.; Courgneau, C.; Guinault, A.; Domenek, S.; Barrier Properties of Poly(lactic acid) and its Morphological Changes Induced by Aroma Compound Sorption. Polym. Int. 2001, 59, 818-826.

[19] Sawada, H.; Takahashi, Y.; Miyata, S.; Kanehashi, S.; Sato, S.; Nagai, K.; Gas Transport Properties and Crystalline Structures of Poly(lactic acid) Membranes. Trans. Mat. Res. Soc. Japan 2010, 35, 241-246.

[20] Drieskens, M.; Peeters, R.; Mullens, J.; Franco, D.; Lemstra, P. J.; Hristova-Bogaerds, D. G.; Structure versus Properties Relationship of Poly(lactic acid). I. Effect of Crystallinity on Barrier Properties. J. Polym. Sci. B 2009, 47, 2247-2258.

[21] Guinault, A.; Sollogoub, C.; Ducruet, V.; Domenek, S.; Impact of Crystallinity of Poly(lactide) on Helium and Oxygen Barrier Properties. Eur. Polym. J. 2012, 48, 779-788.

[22] Courgneau, C.; Domenek, S.; Lebossé, R.; Guinault, A.; Avérous, L.; Ducruet, V.; Effect of Crystallization on Barrier Properties of Formulated Polylactide. Polym. Int. 2012, 61, 180-189.

[23] Sato, S.; Nyuui, T.; Matsuba, G.; Nagai, K.; Correlation between Interlamellar Amorphous Structure and Gas Permeability in Poly(lactic acid) Films. J. Appl. Polym. Sci. 2014, 131, 40626.

[24] Fernandes Nassar, S.; Guinault, A.; Delpouve, N.; Divry, V.; Ducruet, V.; Sollogoub, C.; Domenek, S.; Multi-scale Analysis of the Impact of Polylactide Morphology on Gas Barrier Properties. Polymer 2017, 108, 163-172.

[25] del Río, J.; Etxeberria, A.; López-Rodríguez, N.; Lizundia, E.; Sarasua, J. R.; A PALS Contribution to the Supramolecular Structure of Poly(L-lactide). Macromolecules 2010, 43, 4698-4707.

[26] Bai, H.; Huang, C.; Xiu, H.; Zhang, Q.; Deng, H.; Wang, K.; Chen, F.; Fu, Q.; Significantly Improving Oxygen Barrier Properties of Polylactide via Constructing Parallel-aligned Shish-kebab-like Crystals with Well-Interlocked Boundaries. Biomacromolecules 2014, 15, 1507-1514.

[27] Arnoult, M.; Dargent, E.; Mano, J.F.; Mobile Amorphous Phase Fragility in Semi-Crystalline Polymers: Comparison of PET and PLLA. Polymer 2007, 48, 1012–1019.

[28] Sarasua, J. R.; Prud´Homme, R. E.; Wisniewski, M.; Le Borgne, A.; Spassky, N.; Crystallization and Melting Behavior of Polylactides. Macromolecules 1998, 31, 3895-3905.

[29] Sarasua, J. R.; Arraiza, A. L., Balerdi, P.; Maiza, I.; Crystallinity and Mechanical Properties of Optically Pure Polylactides and their Blends. Polym. Eng. Sci. 2005, 45, 745-753.

[30] Righetti, M.C.; Tombari, E.; Crystalline, Mobile Amorphous and Rigid Amorphous Fractions in Poly(L-lactic acid) by TMDSC. Thermochim. Acta. 2011, 522, 118–127.

[31] Tsuji, H.; Ikada, Y.; Stereocomplex Formation between Enantiomeric Poly(lactic acid)s. XI. Mechanical Properties and Morphology of Solution-Cast Films. Polymer 1999, 40, 6699-6708.

[32] Zhang, J.; Sato, H.; Tsuji, H.; Noda, I.; Ozaki, Y.; Infrared Spectroscopic Study of CH3..O=C Interaction during Poly(L-lactide):Poly(D-lactide) Stereocomplex Formation. Macromolecules 2005, 38, 1822-1828.

[33] Garcia, A.; Iriarte, M.; Uriarte, C.; Iruin, J. J.; Etxeberria, A.; del Rio, J.; Antiplasticization of a Polyamide: a Positron Annihilation Lifetime Spectroscopy Study. Polymer 2004, 45, 2949-2957.

[34] Eldrup, M.; Lightbody, D.; Sherwood, J.N.; The Temperature Dependence of Positron Lifetimes in Solid Pivalic Acid. Chem. Phys. 1981, 63, 51-58.

[35] Nakanishi, H.; Wang, S.J.; Jean, Y.C. In Positron Annihilation Studies of Fluids, Sharma, C., Ed.; World Scientific: Singapore, 1988, p 285.

[36] Wang, Y. Y.; Nakanishi, H.; Jean, Y. C.; Sandreczki, T. C.; Positronium Formation at Free-Volume Sites in the Amorphous Regions of Semicrystalline PEEK. J. Polym. Sci. B 1990, 27, 1419-1424.

[37] Wang, C. L.; Hirade, T.; Maurer, F. H. J.; Eldrup, M.; Pedersen, N. J., Free-Volume Distribution and Positronium Formation in Amorphous Polymers: Temperature and Positron-Irradiation-Time Dependence. J. Chem. Phys. 1998, 108, 4654-4661.

[38] Zuza, E.; Ugartemendia, J. M.; Lopez, A.; Meaurio, E.; Lejardi, A.; Sarasua, J. R. Glass Transition Behavior and Dynamic Fragility in Polylactides Containing Mobile and Rigid Amorphous Fractions. Polymer 2008, 49, 4427-4432.

[39] Crank, J. S.; The mathematics of diffusion, 2nd ed.; Clarendon Press: Oxford, 1975.

[40] Miguel, O.; Iruin, J. J.; Fernandez-Berridi, M. J.; Survey on Transport Properties of Liquids, Vapors, and Gases in Biodegradable Poly(3-hydroxybutyrate) (PHB). J. Appl. Polym. Sci. 1997, 64, 1849-1859.

[41] Gonzalez, A.; Eceolaza, S.; Etxeberria, A.; Iruin, J. J.; Diffusivity of Ethylene and Propylene in Atactic and Isotactic Polypropylene: Morphology Effects and Free-Volume Simulations. J. Appl. Polym. Sci. 2007, 104, 3871-3878.

[42] Sangroniz, A.; Chaos, A.; Garcia, Y. M.; Fernández, J.; Iriarte, M.; Etxeberria, A.; Improving the Barrier Character of Polylactide/Phenoxy Immiscible Blend Using Poly(lactide-co-ε-caprolactone) Block Copolymer as a Compatibilizer. J. Appl. Polym. Sci. 2017, 134, 45396.

[43] Lizundia, E.; Vilas, J.L.; Sangroniz, A.; Etxeberria, A.; Light and Gas Barrier Properties of PLLA/Metallic Nanoparticles Composite Films. Eur. Polym. J. 2017, 91, 10-20.

[44] Delpouve, N.; Arnoult, M.; Saiter, A.; Dargent, E.; Saiter, J.M.; Evidence of Two Mobile Amorphous Phases in Semicrystalline Polylactide Observed from Calorimetric Investigations. Polym. Eng. Sci. 2014, 54, 1144-1150.

[45] Saiter, A.; Delpouve, N.; Dargent, E.; Oberhauser, W.; Conzatti, L.; Cicogna, F.; Passaglia, E.; Probing the Chain Segment Mobility at the Interface of Semi-Crystalline Polylactide/Clay Nanocomposites. Eur. Polym. J. 2016, 78, 274-289.

[46] Fernandes–Nassar, S.; Domenek, S.; Guinault, A.; Stoclet, G.; Delpouve, N.; Sollogoub, C.; Structural and Dynamic Heterogeneity in the Amorphous Phase of Poly(L,L–lactide) Confined at the Nanoscale by the Coextrusion Process. Macromolecules 2018, 51, 128–136.

[47] Lopez-Rodriguez, N.; Martinez de Arenaza, I.; Meaurio, E.; Sarasua, J. R.; Improvement of Toughness by Stereocomplex Crystal Formation in Optically Pure Polylactides of High Molecular Weight. J. Mech. Behav. Biomed. Mater. 2014, 37, 219-25.

[48] Kanehashi, S.; Nakagawa, T.; Nagai, K.; Duthie, X.; Kentish, S.; Stevens, G.; Effects of Carbon Dioxide-Induced Plasticization on the Gas Transport Properties of Glassy Polyimide Membranes. J. Membr. Sci. 2007, 298, 147-155.